

Stanton, S. G., Kantor, A. B., Petrossian, A., & Owicki, J. C. (1984) *Biochim. Biophys. Acta* 776, 228.  
 Sveda, M. M., Markoff, L. J., & Lai, C.-J. (1984) *J. Virol.* 49, 223.  
 Verhoeven, M., Fang, R., Min Jou, W., Devos, R., Huyle-

broeck, D., Saman, E., & Fiers, W. (1980) *Nature (London)* 286, 771.  
 Whiteley, N. M., & Berg, H. C. (1974) *J. Mol. Biol.* 87, 541.  
 Wilson, I. A., Skehel, J. J., & Wiley, D. C. (1981) *Nature (London)* 289, 366.

## Physicochemical Characterization of the $\alpha$ -Peptide of the Sodium Channel from Rat Brain<sup>†</sup>

Lawrence W. Elmer,<sup>‡</sup> Bonnie J. O'Brien, Thomas J. Nutter, and Kimon J. Angelides\*

Department of Neuroscience and Center for Neurobiological Sciences, University of Florida, College of Medicine, Gainesville, Florida 32610

Received March 6, 1985; Revised Manuscript Received July 10, 1985

**ABSTRACT:** The  $\alpha$ -peptide of the rat brain sodium channel of apparent molecular weight 260K has been purified to homogeneity in order to determine its structural and chemical properties. By negative-stain electron microscopy, the molecule morphology of the solubilized channel protein appears as a stack of disks or rouleaux whose dimensions are 40 Å × 200 Å. Measurement of the secondary structure by circular dichroism shows that the  $\alpha$ -peptide is a conformationally flexible polypeptide that contains mostly  $\beta$ -sheet and random-coil in mixed detergent-phospholipid micelles and folds into a conformation that has approximately 65%  $\alpha$ -helix after reconstitution into phosphatidylcholine vesicles. Preparative polyacrylamide gel electrophoresis was used to obtain a chemically homogeneous peptide to analyze the amino acid and carbohydrate composition. The amino acid composition shows a reasonably high content of acidic amino acids with no striking excess of hydrophobic amino acids, while carbohydrate analyses show that carbohydrate is 31% by weight of the protein with sialic acid representing over 50% of the total carbohydrates. The high  $\alpha$ -helical content, the amino acid composition, and the large carbohydrate mass are similar to those of the eel electroplax sodium channel and appear to be general features of the sodium channels which have been analyzed structurally and chemically to date.

**P**ropagation of the action potential in nerve and muscle cells is the result of a transient increase in the membrane permeability to sodium ions. These permeability changes are controlled by a transmembrane protein channel, the sodium channel, which is gated to a sequence of resting, opened, and closed states during excitation. Although the electrical properties of this membrane channel have been extensively investigated, only until relatively recently has the molecular composition of this system been described. Current evidence from photoaffinity labeling, radiation inactivation, and purification and reconstitution suggests that sodium channels from eel electroplax (Agnew et al., 1978, 1983), rat brain synaptosomes (Beneski & Catterall, 1980; Hartshorne & Catterall, 1981; Barhanin et al., 1983a,b), and rat sarcolemma (Barchi et al., 1984) are composed of a glycoprotein of  $M_r \sim 260K$  ( $\alpha$ ). The sodium channel isolated from mammalian brain includes additional subunits of  $M_r$  39K ( $\beta_1$ ) and 37K ( $\beta_2$ ) in which  $\beta_2$  is apparently linked to  $\alpha$  by disulfide bonds (Hartshorne et al., 1982). However, the functional substructure of the rat brain sodium channel complex, as revealed by radiation inactivation techniques, is an assembly composed of only the 260-kilodalton (kDa)<sup>1</sup> ( $\alpha$ ) and 39-kDa ( $\beta_1$ ) polypeptide components (Barhanin et al., 1983b; Angelides et al., 1985). These proteins appear to be sufficient in mediating

transmembrane ion flux after reconstitution into lipid bilayers and respond to pharmacological agents in a fashion similar to sodium channels in situ (Tamkun & Catterall, 1981; Weigle & Barchi, 1982; Rosenberg et al., 1983; Hartshorne et al., 1985). Recently, highly purified sodium channels isolated from rat brain and eel electroplax consisting of only the  $\alpha$ -peptide have been shown by single-channel techniques to be pharmacologically- and voltage-regulated after reconstitution into defined lipid membranes (Hanke et al., 1984; Rosenberg et al., 1984). This indicates that the 260-kDa peptide is unique in that many of the conducting and regulatory functions of the channel are associated with a single polypeptide chain.

Through the application of fluorescent techniques, some structural information has appeared describing the arrangement of the neurotoxin receptor sites of the in situ channel (Angelides & Nutter, 1983a,b). These measurements have shown that many of the functional sites on the  $\alpha$  component are topologically distant and therefore must communicate through alterations in the polypeptide matrix of a conformationally flexible  $\alpha$ -chain (Darbon & Angelides, 1984; Angelides & Brown, 1984).

<sup>†</sup>Supported by a research grant from the National Institutes of Health (NS 18268).

\*Correspondence should be addressed to this author.

<sup>‡</sup>Recipient of an M.D./Ph.D. fellowship from the University of Florida.

<sup>1</sup> Abbreviations: Hepes, 4-(2-hydroxyethyl)-1-piperazineethanesulfonic acid; STX, saxitoxin; TTX, tetrodotoxin; SDS, sodium dodecyl sulfate; MAP-2, microtubule-associated protein 2; NF1, -2, and -3, neurofilament triplet proteins 1, 2, and 3, respectively; Cx II, toxin II from *Centruroides suffusus suffusus*; kDa, kilodalton(s); Tris-HCl, tris(hydroxymethyl)aminomethane hydrochloride; WGA, wheat germ agglutinin.

Because of its central role in ion conduction, this paper reports on the physical and chemical characteristics of the sodium channel  $\alpha$ -protein isolated and purified from rat brain. The morphological and structural properties of the channel protein in mixed detergent micelles and after reconstitution into lipid vesicles are described. The circular dichroism spectra show that the  $\alpha$ -protein is a conformationally flexible protein that contains mostly  $\beta$ -sheet and random-coil structures in mixed detergent-phospholipid micelles and acquires predominantly  $\alpha$ -helix after reconstitution into pure egg phosphatidylcholine vesicles. The secondary structures of the rat brain and the eel electroplax channels are similar and suggest comparable folding of the channel polypeptide in phospholipid bilayers. Electron microscopy of the purified protein shows a rod-shaped structure of dimensions  $40 \text{ \AA} \times 200 \text{ \AA}$  with ribbonlike helices. Analysis of the amino acid composition of the rat brain channel protein shows similarities to the eel electroplax channel with no striking excess of hydrophobic amino acids while carbohydrate analyses show a high content of sialic acid.

#### MATERIALS AND METHODS

**Materials.** Triton X-100, chicken egg yolk phosphatidylcholine (type III-E), DEAE-Sephadex A-25, CNBr-activated Sepharose 4B, wheat germ agglutinin, Hepes, and the protease inhibitors pepstatin A, leupeptin, iodoacetamide, 1,10-phenanthroline, and phenylmethylsulfonyl fluoride were all obtained from Sigma Chemical Co.; hydroxylapatite (Bio-Gel HTP) was purchased from Bio-Rad Laboratories. [ $^3\text{H}$ ]-Saxitoxin was obtained from the Toxicology Study Section, National Institutes of Health, and had a specific radioactivity of 2.6 dpm/fmol. All other reagents were of the highest commercial grade quality available. Solutions were made with deionized distilled water. All preparative buffers contained the following cocktail of protease inhibitors: phenylmethanesulfonyl fluoride (1 mM), iodoacetamide (1 mM), 1,10-phenanthroline (1 mM), pepstatin A (1  $\mu\text{M}$ ), and leupeptin (1  $\mu\text{M}$ ).

**Preparation of Brain Membranes.** Lysed P3 membranes from rat brain were prepared as described by Catterall et al. (1979). Thirty to forty rats were killed by carbon dioxide inhalation. Their brains were rapidly removed, minced, and homogenized in ice-cold 0.32 M sucrose containing 5 mM Tris-HCl, pH 7.4, and a cocktail of the five protease inhibitors. The finally lysed P3 pellet was resuspended in a final volume of 120 mL in a solution containing 200 mM KCl and 10 mM Hepes adjusted to pH 7.4 with Tris base, and the five protease inhibitors, to a final concentration of 16–18 mg of protein/mL. The resuspended P3 pellet was used immediately or stored frozen at  $-70^\circ\text{C}$  for no longer than 1 month.

**[ $^3\text{H}$ ]Saxitoxin Binding Assays.** [ $^3\text{H}$ ]STX binding to synaptosomes and lysed P3 membranes was measured by a filtration assay as described (Catterall et al., 1979). Nonspecific binding was measured in the presence of 1  $\mu\text{M}$  TTX and was subtracted from the total binding data.

Binding assays of detergent extracts and column fractions were measured by rapid gel filtration through 2.0 mL of Sephadex G-50 in a 3.0-mL plastic syringe (Levinson et al., 1979). Detergent extracts and column chromatographic fractions were assayed by removing an aliquot and adding it to a medium composed of 100 mM choline chloride, 20 mM Hepes (adjusted to pH 7.4 with Tris base), 0.2% Triton X-100, 0.04% egg phosphatidylcholine, 0.1 mM  $\text{CaCl}_2$ , and 18 nM [ $^3\text{H}$ ]STX to a total volume of 250  $\mu\text{L}$ . After incubation for 10 min at  $4^\circ\text{C}$ , 200  $\mu\text{L}$  of the reaction mixture was layered onto the Sephadex column and centrifuged at 1000g for 1 min.

The eluate containing the void volume of the column was collected and counted for bound tritium by scintillation counting. Nonspecific binding was determined in the presence of 1  $\mu\text{M}$  TTX and subtracted from the total binding in all the data shown. Binding of [ $^3\text{H}$ ]STX to the reconstituted channel was also performed by the gel filtration method.

**Solubilization, Purification and Reconstitution of the Sodium Channel.** The procedure described by Hartshorne & Catterall (1984) was used without modification to purify the sodium channel protein. The channel was solubilized in Triton X-100 and stabilized by the addition of phosphatidylcholine and 10 mM  $\text{CaCl}_2$ . The channel is purified by sequential chromatography by ion exchange on DEAE-Sephadex, absorption chromatography on hydroxylapatite, and affinity chromatography on wheat germ agglutinin-Sepharose 4B, followed by sedimentation through sucrose gradients.

Eluted column fractions were assayed for protein by the conductivity and by their ability in the solubilized form to bind [ $^3\text{H}$ ]STX. Those fractions eluting with conductivities between 8 and 13  $\text{m}\Omega^{-1}$  at  $4^\circ\text{C}$  from the DEAE-Sephadex column and between 16 and 25  $\text{m}\Omega^{-1}$  at  $4^\circ\text{C}$  from the hydroxylapatite step were collected for further purification.

Wheat germ agglutinin was coupled to CNBr-activated Sepharose 4B at a density of 10 mg of lectin/mL of hydrated resin. The eluate from the hydroxylapatite column was further purified by chromatography on 10 mL of this resin in a  $1.0 \times 15 \text{ cm}$  column. The column was eluted with a solution of 0.4 M NaCl, 20 mM Hepes/Tris, pH 7.4, 10 mM  $\text{CaCl}_2$ , 0.1% (w/v) Triton X-100, and 0.025% (w/v) phosphatidylcholine containing 50 mM *N*-acetylglucosamine at a flow rate of 0.5 mL/min. Fractions of 1.0 mL were collected and assayed for protein and for the ability to bind [ $^3\text{H}$ ]STX. The four fractions with the highest specific activities were saved for further purification. The final purification step was sedimented through linear 5–20% sucrose gradients containing 50 mM NaCl, 10 mM Hepes/Tris, pH 7.4, 10 mM  $\text{CaCl}_2$ , 0.1% Triton X-100 (w/v), and 0.025% (w/v) phosphatidylcholine. One milliliter of the eluate from the peak of the wheat germ agglutinin column was carefully layered onto each of four sucrose gradients and sedimented for 4 h at 215000g in a Ti 50 vertical rotor. The gradients were fractionated by withdrawal from the bottom of the tube and by pumping into a fraction collector. The protein concentration of each fraction was determined by Peterson's assay (Peterson, 1979), and the amount of [ $^3\text{H}$ ]STX binding was measured in duplicate assays by rapid gel filtration.

Fractions having the highest specific STX binding activity (25–40  $\mu\text{g}/\text{mL}$ ) were reconstituted into egg phosphatidylcholine (Sigma type V-E, 99% purity) vesicles at a final concentration of 1.75% Triton X-100 (w/v) and 0.85% (w/v) phosphatidylcholine. The lipid to protein ratio was varied between 3400:1 and 2100:1. To remove the detergent, 0.2 g/mL prewashed Bio-Beads SM2 was added, and the sample was rotated overnight at  $4^\circ\text{C}$ . The Bio-Beads were replaced by an identical volume of fresh Bio-Beads, and the sample was rotated an additional 2 h at  $4^\circ\text{C}$ . The Bio-Beads were then removed by filtration.

**Electron Microscopy.** Negative staining was performed by application of an aliquot of the peak STX fraction from the sucrose density gradient to a 400-mesh formvar carbon-coated grid. The solution was allowed to adhere to the grid for 30 s, blotted to remove excess solution, and then stained with one drop of 1% aqueous uranyl acetate at pH 4.5 for 30 s. In some experiments, the sample (at pH 7.4) was acidified to pH 5.0 with an equal volume of 0.12 M acetic acid for 10 s, followed

by staining with 1% aqueous uranyl acetate at pH 4.5. Excess stain was absorbed with filter paper and then air-dried prior to examination in a Joel 100 CX electron microscope operated at 80 kV.

**Circular Dichroism Spectroscopy.** Circular dichroism spectra of the solubilized and reconstituted channel protein were recorded with a Jasco J-500 spectropolarimeter equipped with a variable-detector geometry which allowed variation of the acceptance half-angles from  $1^\circ$  to  $90^\circ$ . Most spectra were obtained with the photomultiplier tube placed directly adjacent to the sample cell, resulting in a total acceptance angle of  $90^\circ$ . The instrument was calibrated with *d*(+)-10-camphorsulfonic acid at 290 and 192.5 nm (Chen & Yang, 1977). The calibration at lower wavelengths was also checked with sperm whale myoglobin. Measurements were made at  $25^\circ\text{C}$  by using a calibrated 0.01-cm path-length cell. Spectra were generally accumulated at a scanning speed of 2 nm/min and a time constant of 8–16 s over the wavelength range of 300–190 nm. All samples were scanned 4 or 5 times, and the spectra used for computations represent an average of the scans. Several preparations of the solubilized and reconstituted  $\text{Na}^+$  channel were examined. UV absorption spectra from 400 to 190 nm were obtained with a Cary 210 recording spectrophotometer equipped with a thermostated cell holder and with the cell placed adjacent to the detector. Spectra were obtained at a scanning rate of 0.2 nm/s.

Uncorrected mean residue ellipticities were calculated on the basis of a mean residue weight of 116 as determined from amino acid analysis of the purified protein (see below). The concentrations of the specimens used in CD experiments were measured by Peterson's assay (Peterson, 1977) with the biuret correction factor and by direct amino acid analysis determinations. The circular dichroism data were then corrected for optical artifacts by a method that assumes that the measured absorption of a particulate sample is the sum of the absorptions of the chromophores modified by light scattering and absorption flattening effects (Wallace & Mao, 1984). The magnitude of the apparent absorption due to light scattering [ $A_s(\lambda)$ ] was measured in a region of the spectrum where the chromophore absorption is negligible (400–310 nm) and was then extrapolated to lower wavelengths according to  $A_s(\lambda) = k\lambda^{-n}$  where  $k$  and  $n$  are constants and  $\lambda$  is the wavelength. From this, the scattering contribution to the measured absorbance of the suspension was subtracted. To obtain the absorbance of a dispersed, uniform distribution of the channel protein, the absorption spectrum [ $A_{\text{sol}}(\lambda)$ ] of the reconstituted channel was measured after solubilization with 1.8% Triton X-100. Since the absorbances of the reconstituted and solubilized channel protein were measured and the absorbance at each wavelength due to light scattering, a flattening quotient,  $Q(\lambda)$ , was obtained and used to correct for distortions in the CD spectrum arising from differential absorption flattening (Wallace & Mao, 1984). The flattening corrections of the ellipticities were then computed by assuming that differential absorption flattening is identical for left and right circularly polarized light.

In some of the CD spectra obtained, distortions due to differential light scattering or absorption flattening in the CD spectra were minimized by reconstitution of the channel protein into small unilamellar vesicles (Mao & Wallace, 1984). Reconstituted channel vesicles were separated according to size on a Sepharose CL-2B column ( $1.8 \times 14.0$  cm) that had been calibrated with latex spheres, and vesicles eluting between 200 and 350 Å were collected. This was confirmed by the identity of the CD spectra taken with large and small acceptance angles

and by reconstituting at an average ratio of one channel per vesicle. Under these conditions, the sample is equivalent to a dispersed solution and the absorption flattening minimized (Mao & Wallace, 1984).

Following correction for optical artifacts, data points at 1-nm intervals between 190 and 250 nm were computer-fit to a reference set by a constrained linear least-squares method. The program searches for percentages of  $\alpha$ -helix,  $\beta$ -structure,  $\beta$ -turns, and aperiodic structure from a reference set (Chang et al., 1978). The reference data set used was derived from 15 water-soluble proteins of known crystallographic structure. As the magnitude of the helix spectrum is a function of helical length, helical length could also be put in as an input variable. The quality of each computer fit was evaluated by calculating a normalized standard deviation for each curve according to Mao et al. (1982).

**Analytical and Preparative Gel Electrophoresis.** Column fractions from the purification of the sodium channel protein were analyzed by SDS-polyacrylamide gel electrophoresis on linear 4–15% acrylamide gradients containing 0.1% SDS with a 3% stacking gel in the discontinuous gel system of Laemmli (1970). The concentration of methylenebis(acrylamide) in all gels was 2.7% of the total acrylamide concentration. In some cases, 1 mM iodoacetamide was added and the sample alkylated for 30 min under nitrogen at room temperature. Molecular weights of the protein bands were estimated by comparison with the migration of the following proteins of known molecular weights: MAP-1, 350 000; MAP-2, 265 000 and 255 000; fodrin, 250 000 and 240 000, a neuronal cytoskeleton preparation containing the neurofilament triplet proteins NF1 (210 000), NF2 (173 000), and NF3 (68 500) (Scott et al., 1985);  $\alpha$ - and  $\beta$ -tubulin, 57 000 and 55 000, respectively; actin, 41 350; and *Escherichia coli* pyruvate dehydrogenase multienzyme complex, consisting of pyruvate dehydrogenase (E1) (96 000), lipoyl acetyltransferase (E2), (76 000), and lipoamide dehydrogenase (E3) (55 000). After electrophoresis, the proteins were fixed in methanol/water (50:50) and stained with ammoniacal silver (Wray et al., 1981).

Preparative SDS gel electrophoresis was performed in a BRL preparative unit using the electrophoretic system of Laemmli (1970). The separation was performed on a 4% polyacrylamide separating gel ( $1.8 \times 7$  cm) with a 3% stacking gel ( $1.8 \times 2$  cm). The peak fractions from the wheat germ agglutinin step were combined and reduced in volume to 1.0 mL by ultrafiltration on an Amicon XM-100 membrane. A 1.0-mL sample was loaded and the sample electrophoresed at less than 2 W for approximately 12 h. One-milliliter fractions were collected at a flow rate of 6 mL/h. Fractions were assayed by analytical electrophoresis in the Laemmli system with 4–15% linear acrylamide separating gels. The  $\alpha$ -peptide-containing fractions were identified by silver staining, pooled, lyophilized, and redissolved in sample buffer containing 0.02% SDS. The material was exhaustively dialyzed against 50 mM ammonium acetate, pH 6.5, containing 0.02% SDS for 72 h. Samples from the preparative gel containing no proteins were processed in an identical fashion in order to ascertain the decrease in glycine which is a component of the eluting buffer.

Amino acid analyses of the purified  $\alpha$ -peptide were performed by Dr. John Shiveley, Division of Immunology, City of Hope, Duarte, CA, after hydrolysis in 6 N HCl containing 0.02%  $\beta$ -mercaptoethanol at  $110^\circ\text{C}$  under reduced pressure for 24 h (Yuan et al., 1982). Some samples were processed by using a two-column system which analyzes glucosamine, galactosamine, and amino acids (Del Valle & Shiveley, 1979).

Table I: Sodium Channel Purification

purification step	protein		sp act. (pmol of [ $^3$ H]STX/mg)	x-fold purification
	mg	%		
Triton X-100 extract	1145 $\pm$ 157	100	5.1 $\pm$ 0.7	1.0
DEAE-Sephadex A-25	43.7 $\pm$ 11.6	3.8	102 $\pm$ 12	20.0
hydroxylapatite	5.8 $\pm$ 0.2	0.51	187 $\pm$ 28	36.6
WGA/Sepharose 4B	0.66 $\pm$ 0.03	0.058	832 $\pm$ 99	163.0
sucrose gradient	0.13 $\pm$ 0.03	0.011	2261 $\pm$ 416	443.3

Values reported are from a total of 13 determinations on 4 separately purified samples. In some samples, the amount of protein to be analyzed was determined by Peterson's modification of the Lowry method using bovine serum albumin as a standard. The corresponding biuret correction factors were obtained by comparison of the Peterson method and the material balance for the protein by amino acid analysis. The Peterson procedure overestimates the protein concentration by 1.37 times.

Carbohydrate analyses were performed by gas-liquid chromatography according to Clamp et al. (1972). Material purified by preparative SDS gel electrophoresis was dialyzed extensively against distilled water containing 0.02% SDS. Aliquots of protein were mixed with 2  $\mu$ g of mannitol (as an internal standard) and lyophilized. The dry residue was dissolved in 1.5 M HCl in anhydrous methanol and then hydrolyzed at 110  $^{\circ}$ C for 24 h under vacuum. The solution was dried under a stream of nitrogen gas and derivatized with acetic anhydride and then with Tri-Sil (Pierce Chemical Co.). Derivatized samples were injected into a 3 mm  $\times$  2 m column packed with 3.8% OV-1 mounted in a Perkin-Elmer GC-7A gas chromatograph. The column was programmed with a temperature gradient of 120–250  $^{\circ}$ C at 2  $^{\circ}$ C/min, and eluted compounds were monitored with a flame ionization detector. Compounds were identified by comparing retention times with those of identically treated standard sugars. The mass of each sugar was determined by comparing the areas under the peak with that of a known amount of the standard.

## RESULTS

**Purity of the Sodium Channel Protein.** The sodium channel from rat brain was purified by sequential chromatography on DEAE-Sephadex, hydroxylapatite, and wheat germ agglutinin/Sepharose 4B followed by velocity sedimentation through sucrose gradients. The four best preparations gave an average specific activity of 2261  $\pm$  416 pmol/mg of protein compared to a specific activity of 5.1  $\pm$  0.7 pmol/mg of protein for the detergent extract or a 400-fold purification. Other preparations have shown specific activities that have exceeded 1800 pmol/mg of protein. Table I summarizes the purification procedures, yields, and specific activities for each of these steps.

The correlation of the high STX binding and purification of the sodium channel protein was also followed by SDS gel electrophoresis. Figure 1 shows an analytical gel of the peak fractions from each of the purification steps. The HTP fraction could not be readily examined because of the high potassium content in the eluting buffer. As can be seen, the purification scheme eliminates a large number of proteins to yield in the final step a diffusely staining protein with an apparent molecular weight of 260K. The most persistent contaminant that we have observed is a protein of molecular weight 150K. Most of this polypeptide could be eliminated

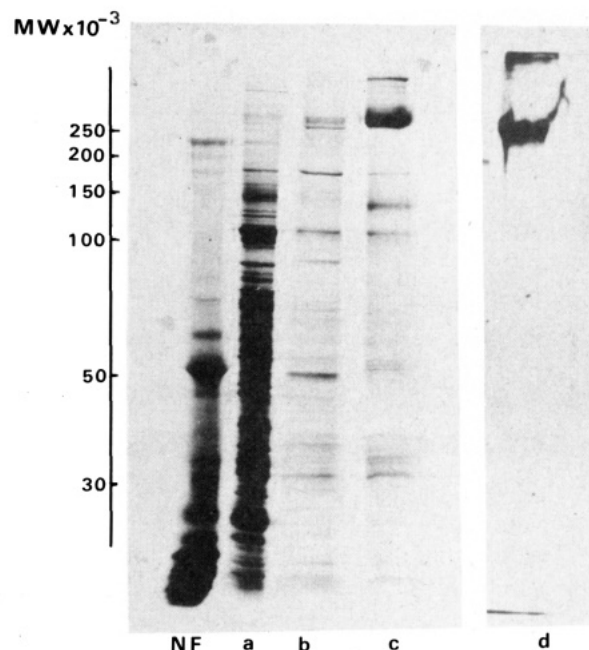


FIGURE 1: Analytical SDS-polyacrylamide gel electrophoresis of the rat brain sodium channel purification. Approximately 5  $\mu$ g from the peak [ $^3$ H]STX binding fractions of each chromatographic step and from the sucrose gradient was applied to a 4–15% linear polyacrylamide gel and stained with ammoniacal silver. NF, a neuronal cytoskeleton preparation consisting of MAP-2 proteins (265 and 255 kDa), fodrin (250 and 240 kDa), NF1 (210 kDa), NF2 (173 kDa), NF3 (68.5 kDa),  $\alpha$ - and  $\beta$ -tubulin (57 and 55 kDa, respectively), and actin (41 350 kDa); lane a, Triton X-100 detergent extract; lane b, DEAE-Sephadex step; lane c, wheat germ agglutinin step; lane d, sucrose gradient step. The final product in this preparation had a specific [ $^3$ H]STX binding activity of 2231 pmol/mg of protein.

by differential velocity sedimentation in sucrose, and after centrifugation, only small amounts (<10%) of this 150-kDa impurity were observed in the peak fractions. The gel profile of the final preparation, shown in Figure 1, lane d, indicates that the preparation is essentially homogeneous in that it contains one major polypeptide and binds nearly stoichiometric amounts of STX. However, the precise specific activity and purity based on binding activity are uncertain since a refined molecular weight has not been obtained, and it is inevitable that a certain fraction of channel proteins have lost their ability to bind [ $^3$ H]STX and thus lower the apparent purity based upon the specific binding activity. Starting from 1.1 g of protein of membrane extract, 135  $\mu$ g of sodium channel protein was purified for a final yield of 0.01%.

Highly purified preparations of sodium channels were incorporated into phospholipid vesicles composed of pure egg phosphatidylcholine. When proteoliposomes were formed by detergent removal with Bio-Beads, 40% of the [ $^3$ H]STX binding activity and total protein was lost. However, the recoverable [ $^3$ H]STX binding to the reconstituted channel was saturable with a  $K_d$  of 4.8 nM at 4  $^{\circ}$ C, which is in good agreement with the value obtained by Hartshorne & Catterall (1984). The fraction of reconstituted channels oriented right side out, in which the STX binding site is at the external surface, was measured by disruption of the vesicles with 0.2% Triton X-100 and 0.05% phosphatidylcholine and retitration with 18 nM [ $^3$ H]STX. Data from two separate experiments showed a 1.4-fold increase in the number of [ $^3$ H]STX binding sites, suggesting that about 60% of the channels are oriented with the STX receptor at the external vesicle surface.

**Molecular Morphology of the Purified and Reconstituted Sodium Channel Protein.** Negative-stain electron microscopy was used to examine the morphology of the purified protein



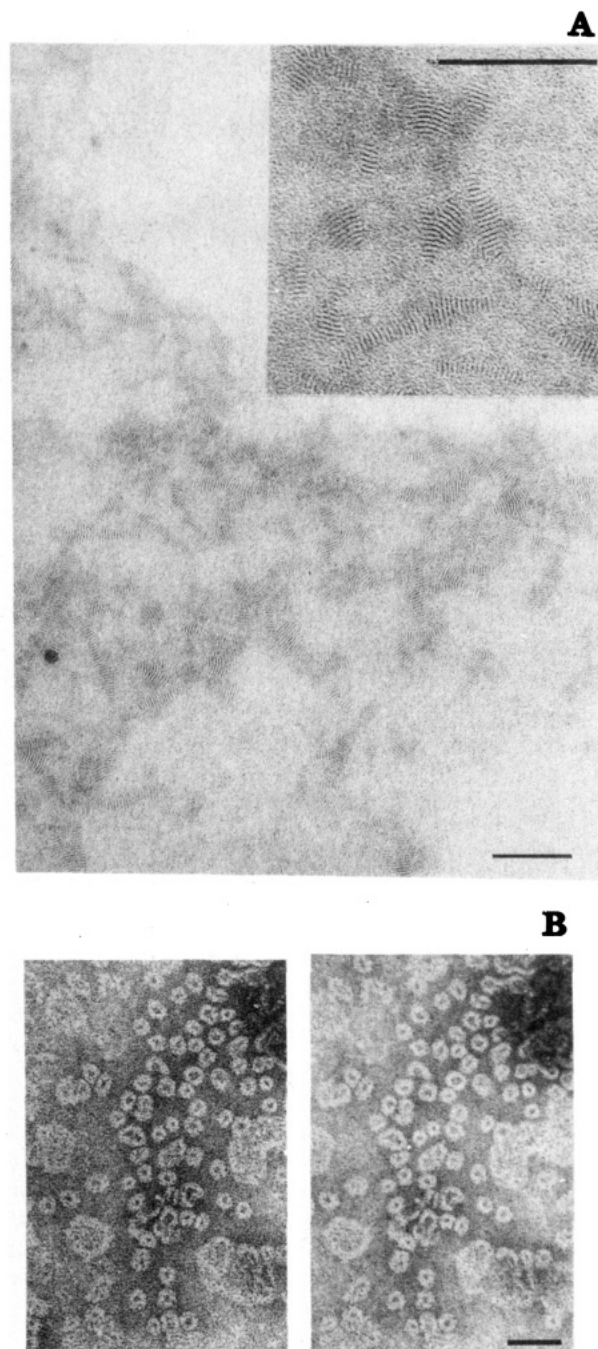


FIGURE 2: Negative-stain electron microscopy of the purified sodium channel protein. The bar in each micrograph is 200 Å. Panel A, a large-field view of clustered, purified, and solubilized channel proteins stained with 1% aqueous uranyl acetate (pH 4.5); panel B, the same sodium channel preparation preacidified to pH 5.0 with acetic acid for 10 s prior to being stained with 1% aqueous uranyl acetate. Stereoscopic pair, 6° and 10° tilts. Here the particles are doughnut shaped with average diameters of 80 Å.

taken from sucrose gradients. Figure 2 shows a series of electron micrographs of a channel preparation with a specific activity of 1740 pmol/mg of protein.

In panel A, in which a large field is examined, the structures observed are clusters of elongated particles characterized by ribbonlike helices. These particles had average dimensions of 40-Å width and 200-Å length. Stereoscopic visualization of these structures has shown that the particles are cylindrical and not flattened disks.

When the solubilized purified channel in elution buffer (pH 7.4) was acidified to pH 5.0 with acetic acid, the same solubilized channel preparation showed strikingly different mor-

phology in the electron microscope (panel B). Here the particles are doughnut shaped with an average diameter of 80 Å. Under each of these conditions, the images presented in Figure 2 are representative of a large number of observations; direct staining led to the presence of several hundred rouleaux in fields from every sample examined whereas treatment with acetic acid prior to staining with uranyl acetate at the lower pH led to the several hundred doughnut-shaped particles.

Many of the negatively stained images of the solubilized channel protein do not exhibit the rigorous morphological similarities that are required for correspondence analysis to be extended to any image subset. This is in sharp contrast to what has been found for other membrane channels such as the acetylcholine receptor (Zingsheim et al., 1984) and bacteriorhodopsin (Henderson & Unwin, 1975) in which the shapes of these proteins are characterized by their regularities.

**Secondary Structure of the Solubilized and Reconstituted Sodium Channel.** Circular dichroism spectroscopy was used to obtain information on the secondary structure of the purified channel reconstituted into small unilamellar vesicles and in mixed detergent-phospholipid micelles (Figure 3). CD spectra of the purified, solubilized, and reconstituted channel are shown in Figure 3. The effects of differential light scattering and absorption flattening on the CD spectra of small unilamellar vesicles are small. For the 350-Å-diameter vesicles and high lipid to protein ratio used in these experiments, correction factors were calculated to be less than 15% of the measured ellipticities at most wavelengths. However, unlike the small unilamellar vesicles which experienced little light scattering and for which the CD measurements at all acceptance angles were similar, an absorption and ellipticity flattening coefficient,  $Q(\lambda)$ , was calculated when larger vesicles were used. The extent of the wavelength dependency of the scattering from a  $\log A_s$  vs.  $\log \lambda$  plot (450–310 nm) yielded a value of 2.8 which can be compared to a theoretical value of 4.0 for small spherical objects. However, it was apparent that the major contribution to the low absorption shown by samples in vesicles was due to absorption flattening since the value of  $A_{sol}(\lambda)$  was about 1.5 times higher than the measured absorbance of the membrane suspension at 195 nm. With the above parameters, typical values for  $Q(\lambda)$  in the large unilamellar vesicles were 0.3–0.4 at 190 nm, indicating that only 60–70% of the intrinsic absorption was shown by the protein.

From the spectra of the channel reconstituted in small unilamellar vesicles and corrected CD spectra with large vesicles, the secondary structure of the  $\text{Na}^+$  channel protein was calculated by using a constrained least-squares program utilizing a reference data set of 15 water-soluble proteins (Chang et al., 1978). The mean residue ellipticities shown in Figure 3A for the reconstituted rat channel protein are  $-21\,233 \text{ deg cm}^2 \text{ dmol}^{-1}$  at 222 nm and  $+43\,321 \text{ deg cm}^2 \text{ dmol}^{-1}$  at 192 nm, indicating a high  $\alpha$ -helical content. Channel phosphatidylcholine vesicles formed with six different lipid to protein ratios (in the ratio range of  $10^3:1$ ) gave nearly identical CD spectra. For a helix length of 26 amino acids, which would be necessary to span a 40-Å-thick bilayer, the CD spectra give secondary structures of 64%  $\alpha$ -helix, 16%  $\beta$ -sheet, 8%  $\beta$ -turn, and 12% random-coil.

To ascertain whether the system had reached equilibrium at the time of measurement, a CD spectrum of the sample was measured after it was allowed to sit overnight at 4 °C. The same CD spectrum was obtained as with the freshly prepared sample, indicating no detectable conformational change occurs with time. When STX or TTX was added to the solubilized

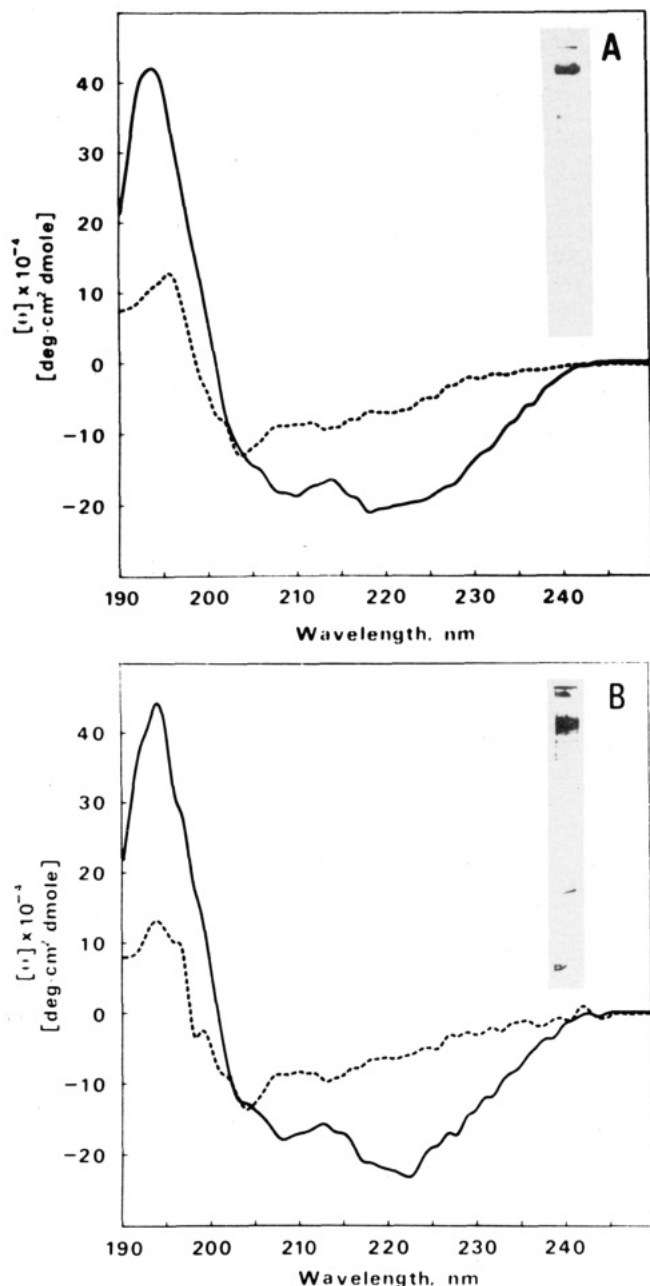


FIGURE 3: (A) Circular dichroism spectra of the solubilized sodium channel (---) and the channel protein reconstituted into small unilamellar phosphatidylcholine vesicles at 25 °C (—). The [ $^3\text{H}$ ]STX binding activity of the channel was 1984 pmol/mg of protein prior to reconstitution and 1053 pmol/mg of protein in the reconstituted vesicles. The purity of the preparation used for CD spectroscopy is shown in the 4–15% polyacrylamide gel strip. The concentration of  $\text{Na}^+$  channel protein was  $1.5 \times 10^{-7}$  M (38  $\mu\text{g}/\text{mL}$ ); the egg phosphatidylcholine lipid to protein ratio was 2400:1. This is the measured CD spectrum corrected for light scattering and absorption flattening effects. The uncorrected spectrum differs in intensity from this by less than 15% at each wavelength. (B) Circular dichroism spectra of the solubilized (---) and reconstituted (—) sodium channel prepared from eel electroplax membranes according to Miller et al. (1983) and reconstituted by the addition of phosphatidylcholine and removal of the detergent by absorption to Bio-Beads SM-2. A SDS–6% polyacrylamide gel of the preparation used for CD is shown in the inset. The specific activity of the purified channel was 1180 pmol/mg of protein after gel filtration chromatography on Sepharose 6B. The protein to lipid ratio was 1:113, in which the channel protein concentration was 115  $\mu\text{g}/\text{mL}$  and the phospholipid concentration was 13  $\mu\text{g}/\text{mL}$ .

or reconstituted channel protein, no changes in the CD spectra were detected, which suggests that no major conformational change, at least at the level of CD spectroscopy, of the channel

Table II: Secondary Structures and Parameters of Sodium Channel Proteins

sample	state	fractional secondary structure <sup>a</sup>			
		$\alpha$	$\beta$	T	R
rat brain $\text{Na}^+$ channel	solubilized	0.32	0.15	0.24	0.29
	reconstituted <sup>b</sup>	0.64	0.16	0.12	0.08
	reconstituted <sup>c</sup>	0.68	0.15	0.11	0.06
eel electroplax $\text{Na}^+$ channel	solubilized	0.38	0.12	0.29	0.21
	reconstituted	0.68	0.17	0.12	0.03

<sup>a</sup> Abbreviations:  $\alpha$ ,  $\alpha$ -helix;  $\beta$ ,  $\beta$ -sheet; T,  $\beta$ -turn; R, random-coil.

<sup>b</sup> Small unilamellar vesicles reconstituted at a lipid to protein ratio of 3100:1. <sup>c</sup> Large vesicles reconstituted at a lipid to protein ratio of 600:1. A flattening quotient was determined and used to correct each spectrum.

occurs with the binding of these ligands.

The CD spectrum for the purified solubilized channel, in which [ $^3\text{H}$ ]STX binding activity is retained, is somewhat different than the spectrum obtained for the channel reconstituted into lipid vesicles (Figure 3A). The more pronounced negative ellipticity observed at 204 nm relative to 222 nm and a reduction in the 192-nm peak are suggestive of more random-coil and a reduced  $\alpha$ -helical content. Calculation of the percentages of secondary structure shows that the percentages of random-coil and  $\beta$ -turn increase to 29% and 24%, respectively, while the percentage of  $\alpha$ -helix decreases to 32%. There appears to be no significant change in the content of  $\beta$ -sheet. This demonstrates that although the overall conformation of the channel protein is altered in the solubilized state as it interacts with detergents, sufficient native conformation at the channel's STX receptor is maintained to reflect preservation of high affinity and capacity for STX binding. The calculated secondary structures of the solubilized and reconstituted sodium channel are summarized in Table II.

CD measurements were also made of the purified and reconstituted sodium channel protein from eel electroplax prepared as described by Miller et al. (1983) to compare the secondary structures of these two proteins. Since the primary structure of this channel has recently been reported (Noda et al., 1984), comparison of the secondary structure by CD provides additional insights into the structure of the mammalian sodium channel protein. The CD results for the eel channel are shown in Figure 3B. The measured ellipticities and shapes of these spectra are very similar to those obtained with preparations of the sodium channel from rat brain and indicate that there are few if any differences between the secondary structures of these two proteins. The calculated percentages of secondary structure of the eel channel are also given in Table II for comparison.

**Preparative Gel Electrophoresis.** To characterize the chemical composition of the  $\alpha$ -peptide of the sodium channel protein, samples from the lectin chromatographic step were further purified by preparative SDS gel electrophoresis. Figure 4 shows a representative profile of the fractions eluting from a 4% polyacrylamide gel column during preparative gel electrophoresis. The composition of the material applied to the column is shown in Figure 1, lane c. As seen in Figure 4, the major impurity of apparent molecular weight 150K elutes between fractions 6 and 8, and the channel protein with an apparent molecular weight of 260K elutes between fractions 20 and 28. Fractions 20–28 were pooled and processed for amino acid and carbohydrate analysis. From 0.5 mg of protein from the wheat germ agglutinin step, typical yields of this peptide were 50  $\mu\text{g}$  of highly purified  $\alpha$ -peptide.

**Amino Acid Composition.** Samples of the  $\alpha$ -peptide purified by preparative gel electrophoresis were analyzed for total

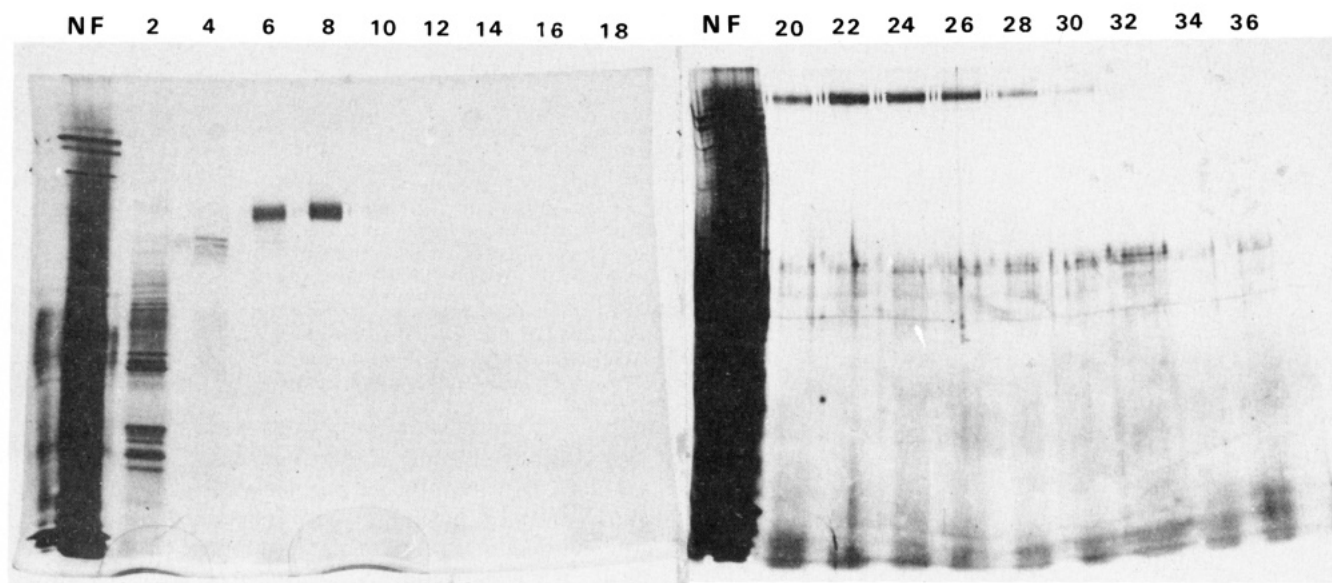


FIGURE 4: Preparative polyacrylamide gel electrophoresis of the sodium channel protein. Electrophoresis was carried out on a 4% polyacrylamide gel at a constant current of 2 mA. One-milliliter fractions were collected at a flow rate of 6 mL/h. An analytical 4–15% polyacrylamide gel of representative fractions which is stained with ammonical silver is shown. Fractions 20–28 were pooled for amino acid and carbohydrate analyses.

Table III: Amino Acid Composition of the Rat Brain Sodium Channel  $\alpha$ -Peptide<sup>a</sup>

amino acid	rat brain Na <sup>+</sup> channel	eel electroplax Na <sup>+</sup> channel <sup>b</sup>
cysteic acid	2.5	ND
CM-Cys	ND <sup>c</sup>	2.0
Asx	10.9	10.1
Thr	4.9	5.0
Ser	7.7	7.1
Glx	11.2	10.8
Pro	4.5	4.7
Gly	5.6	6.5
Ala	6.0	6.0
Val	6.0	5.3
Met	2.1	3.4
Ile	5.4	5.5
Leu	9.7	9.3
Tyr	4.2	2.8
Phe	5.8	5.9
His	0.71	2.8
Trp	1.8	3.5
Lys	6.6	5.0
Arg	4.4	4.3

<sup>a</sup> Mole percent. <sup>b</sup> Miller et al. (1983). <sup>c</sup> Not determined.

amino acid composition as described under Materials and Methods. Combined data from the 13 analyses are given in Table III. Control experiments in which the eluting buffer was also dialyzed showed a complete absence of glycine. Therefore, the amino acid analyses reflect only those residues of the purified peptide. There is not any unusual feature of the amino acid composition that would explain its interaction with SDS nor acidic or polar groups that may contribute to the low electrophoretic free mobility which is observed for this protein (Hartshorne & Catterall, 1984). In Table III, the amino acid compositions of the  $\alpha$ -peptide of the mammalian and eel electroplax sodium channels are compared. In general, there is a striking similarity in the amino acid compositions. Both acidic and basic residues are equally well represented, with Asx and Glx being the most abundant on a mole percent basis in both proteins. Major differences are the low methionine, tryptophan, and histidine contents and higher Tyr content of the rat brain channel. Preliminary sequence analyses of the  $\alpha$ -peptide have indicated that the N-terminus

Table IV: Carbohydrate Composition of the  $\alpha$ -Peptide of the Rat Brain Sodium Channel

carbohydrate	rat brain		eel electroplax <sup>a</sup>	
	% total wt	% of carbohydrate	% total wt	% of carbohydrate
fucose	0.1 $\pm$ 0.1	0.3	0.5	1.5
mannose	1.1 $\pm$ 0.2	3.6	2.4	8.3
galactose	1.2 $\pm$ 0.4	3.9	1.5	5.2
N-acetylglucosamine	12.0 $\pm$ 0.6	38.9	13.3	45.3
sialic acid	16.5 $\pm$ 1.1	53.3	11.8	39.7
total	30.9		29.5	

<sup>a</sup> Miller et al. (1983).

is blocked. Even though slightly different preparative methods were used, the amino acid composition of  $\alpha$ -peptide reported by Grishin et al. (1984) and the amino acid composition reported here are in excellent agreement.

Analysis of the amino acid composition including an internal standard showed that the Peterson protein assay gave 137% of the true value for the protein content. This biuret correction factor was applied to all subsequent carbohydrate and spectroscopic analyses.

**Carbohydrate Composition.** The  $\alpha$ -peptide obtained by preparative gel electrophoresis was analyzed for total carbohydrate composition. Analysis of the carbohydrate composition from three different samples is shown in Table IV. Saccharides detected were mannose, fucose, galactose, N-acetylglucosamine, and sialic acid, the latter two which predominate the carbohydrate profile. From the amount of protein analyzed, the total carbohydrate content was 31% by weight from two preparations. This is similar to the carbohydrate mass determined for the eel electroplax sodium channel whose composition is also given in Table IV for comparison. The only striking difference is the fraction of sialic acid residues found in the mammalian  $\alpha$ -peptide which is about 1.5 times that reported for the eel electroplax channel. In other channel protein preparations, some variation in the degree of glycosylation was observed.

Although the studies of Agnew et al. (1983) have shown that the oligosaccharide chains of the eel sodium channel are



most probably N-linked, we have not been able to unequivocally demonstrate removal of the carbohydrate chains from the rat brain channel either by endoglycosidase H or F or by *N*-glycanase.

## DISCUSSION

Using the methodology developed by Hartshorne & Catterall (1981, 1984) to purify the sodium channel from rat brain and a preparative electrophoretic step, we have characterized the physical and chemical properties of the  $\alpha$ -peptide. In our preparations, a peptide with an apparent molecular weight of 260K is the major species with the absence of smaller peptides in the 40K molecular weight range which would correspond to  $\beta$ 1 and  $\beta$ 2 (Hartshorne et al., 1982). The highest specific activity fractions eluting from sucrose density gradients are of approximately 2300 pmol of STX binding sites per milligram of protein. On the basis of the specific binding activity, the purified sodium channel is 90% of the theoretical value for a pure protein of 260 kDa that binds one STX molecule. The peptide composition, however, suggests that our best preparations are essentially homogeneous and that some channel molecules are not capable of binding toxin. In our highest specific activities, those two smaller molecular weight peptides, designated  $\beta$ 1 and  $\beta$ 2 by Hartshorne et al. (1982), were not observed and may have been lost due to dissociation or proteolysis. The latter is unlikely since protease inhibitors were present throughout the purification and because smaller peptides toward the bottom of analytical SDS gels were not detected. Even through photolabeling experiments with  $\alpha$ - and  $\beta$ -scorpion toxins (Hartshorne et al., 1982; Darbon et al., 1983) and radiation inactivation measurements indicate that the  $\beta$ 1 subunit is part of the functional substructure of the rat brain sodium channel (Angelides et al., 1985), it is possible that it may be derived by partial proteolysis of the large  $\alpha$ -peptide or the  $\beta$ -subunits are structural components of the channel complex associated uniquely with the  $\alpha$ -peptide in neuronal membranes. However, it has been reported that the 260-kDa channel peptide from rat brain without the  $\beta$ -subunits is capable in mediating TTX-sensitive voltage-regulated ion movements after incorporation into planar lipid bilayer membranes (Hanke et al., 1984). This is supported by single-channel recordings with the reconstituted eel electroplax sodium channel preparation consisting of a single 260-kDa polypeptide which conducts sodium ions and responds to pharmacological agents (Rosenberg et al., 1984). Moreover, in both reports, it was shown that the voltage-dependent single-channel conductances were qualitatively and quantitatively similar to those reported for sodium channels in nerve and muscle cells with just the one protein and that the rat brain and eel electroplax channel proteins are not fundamentally different in their physical properties. In the data presented here, we also see that the physical and chemical compositions of the two well-characterized proteins are not fundamentally different.

The appearance of the purified solubilized rat brain sodium channel in negatively stained electron micrographs is similar to those obtained with preparations of the eel electroplax sodium channel. Visualization of these preparations shows a stack of disks or rouleaux whose widths of 40 Å appear to be relatively constant. The length was somewhat more variable within a given complex. The morphologies of these preparations, however, are very similar to those reported for apolipoprotein-alanine III or apolipoprotein A-II complexed with phosphatidylcholine in which stacked disks are characteristic of the phospholipid (Morrisett et al., 1974; Laggner et al., 1979; Massey et al., 1981). Similar morphologies have ar-

tificially been induced by treatment of phospholipid-cholesterol mixtures with bile salts (Howell et al., 1970), by sonication of phosphatidylcholine with apolipoprotein-Gln I (Forte et al., 1971), and in the plasma lipoproteins of humans with biliary obstruction (Hamilton et al., 1971). In all these cases, the formation of the rouleaux appears to be a specific effect mediated by proteins that interact strongly with phosphatidylcholine. Thus, although controls were performed of the eluting buffer alone in which no organized or morphologically distinct structures were observed, the electron micrographs of the solubilized channel shown here and by Ellisman et al. (1982, 1984) raise important questions as to whether these structures actually exist in solution or whether they represent composite morphologies of the lipid-protein interaction, negative staining, drying, or the channel protein morphology.

In order to obtain higher resolution data on the folding and conformation of the native channel protein, we investigated in detail the circular dichroism spectra of the solubilized and reconstituted channel. The CD spectra have revealed important clues to the structure of the channel protein. The single 260-kDa channel polypeptide folds within the membrane such that it assumes substantial  $\alpha$ -helical conformation which is significantly reduced upon solubilization and release of the constraints imposed by the membrane bilayer. Furthermore, the CD spectra and calculated secondary structures are very similar for the eel electroplax and rat brain channel proteins in both the solubilized and reconstituted states. Both preparations contain substantial  $\alpha$ -helix. Other membrane proteins which have shown a high  $\alpha$ -helix content are bacteriorhodopsin (Henderson & Unwin, 1975; Mao & Wallace, 1984) and the mitochondrial  $H^+$ -ATPase proteolipid channel (Mao et al., 1982). For comparison, the secondary structure of the pentameric nicotinic acetylcholine receptor is similar in detergent and in reconstituted proteolipid vesicles and is reported to consist of 38%  $\alpha$ -helix and 29%  $\beta$ -strand (Moore et al., 1974; Yager et al., 1983). The sodium channel protein, however, appears unusual in that folding of the single polypeptide leads to spatially distinct receptors and functional domains (Angelides & Nutter, 1983b; Darbon & Angelides, 1984; Angelides & Brown, 1984; Angelides et al., 1985).

The major limitations to accuracy of the proportions of secondary structure calculated from CD data are errors in estimating the protein concentration, the degree of applicability of the CD reference spectra, and corrections to the spectra for light scattering and absorption flattening effects.

Errors in the channel protein concentration were removed by correction of the biuret factor from the amino acid composition. The uncertainties due to the reference spectra based on water-soluble proteins are indeed appropriate for a protein embedded in the hydrophobic environment of a lipid bilayer. Previous work has shown that the corrected and calculated CD and secondary structure estimates for an integral membrane protein, bacteriorhodopsin, agree quite well with those data obtained by X-ray diffraction, electron microscopy, and model building and suggest that the use of this reference data set for the channel membrane proteins is valid (Mao & Wallace, 1984). Moreover, this reference set tends to give particularly accurate secondary structural estimates for proteins with high  $\alpha$ -helical contents (Provencher & Glockner, 1981), a predominant structural feature in the sodium channel and other membrane proteins.

Although the CD spectra of the sodium channel protein solubilized and reconstituted indicate that the overall conformation of the channel is altered, the conformation of the channel protein about the STX/TTX receptor is preserved to



allow high-capacity binding of these neurotoxins. This preparation, however, is no longer able to bind the voltage-independent  $\beta$ -scorpion toxins such as Csx II (Jover, 1984). At present, it is uncertain whether these changes in secondary structure reflect conformational alterations which lead to loss of binding that may be restricted to a domain of the channel complex. Radiation inactivation experiments have shown that binding of Csx II depends on a receptor structural unit of 43 kDa (Angelides et al., 1985). It is possible that this molecular mass reflects a conformationally flexible domain of the channel protein which is altered after solubilization and removal from specific interactions with the membrane and/or other membrane components.

Although the CD measurements indicate that the channel protein contains extensive  $\alpha$ -helical domains, the amino acid composition does not reflect any preponderance or any unusual excess of amino acids that would be consistent with this organization. The large amounts of glutamic acid could be indicative of coil-coiled sequences.

The extensive carbohydrate mass suggests both structural and functional roles for the carbohydrate. It has been shown that blocking terminal glycosylation in neuroblastoma cells inhibits the expression of [ $^3$ H]STX-titratable sodium channels on the membrane surface (Waechter et al., 1983). The extensive glycosylation may serve to stabilize the  $\alpha$ -peptide of the channel to orient those domains to form specialized structures at the surface of the channel. The carbohydrate content and composition of the mammalian channel are similar to those of the eel electroplax channel and appear to be a general feature of the sodium channels which have been analyzed chemically to date. Alternatively, the extensive glycosylation may serve as a recognition key for the interaction with extracellular matrix elements and other neuronal components and may serve to aid in the organization of this protein within the neuronal membrane.

In summary, in this report we present the morphological, spectroscopic, and chemical characteristics of the rat brain sodium channel protein. The information given here will be important in identifying those structural and conformational features of the channel which dictate its unique functional properties and for elucidating the molecular mechanisms of ion movement through the channel. Many of the physicochemical properties, including the estimation of the secondary structure, are strikingly similar to the major sodium channel polypeptide isolated from the eel electroplax. Since this protein is itself capable of neurotoxin-induced conductances, we anticipate that the rat brain  $\alpha$ -peptide itself forms the ion-conducting pore of the channel. The  $\beta$ -subunits may either be fragments derived from this polypeptide or be structural elements that confer some specialized organization of sodium channels in neuronal membranes.

#### ACKNOWLEDGMENTS

We are grateful to Dr. J. Shiveley and D. Hawkes for the many amino acid analyses they performed. We thank Dr. Bonnie Wallace, Columbia University, for helpful discussions and for kindly providing a preprint of her work, R. Sakurai-san, Okazaki, and Teresa McCord for help with the preparation of the manuscript, and Dr. Susumu Terakawa for preparation of Figure 3 and helpful discussions.

**Registry No.** Sodium, 7440-23-5.

#### REFERENCES

- Agnew, W. S., Levinson, S. R., Brabson, J. S., & Raftery, M. A. (1978) *Proc. Natl. Acad. Sci. U.S.A.* 75, 2606.
- Angelides, K. J., & Nutter, T. J. (1983a) *J. Biol. Chem.* 258, 11958.
- Angelides, K. J., & Nutter, T. J. (1983b) *Biophys. J.* 45, 31.
- Angelides, K. J., & Brown, G. B. (1984) *J. Biol. Chem.* 259, 6117.
- Angelides, K. J., Elmer, L. W., Nutter, T. J., & Kempner, E. S. (1985) *J. Biol. Chem.* 259, 3431.
- Barchi, R. L., Tanaka, J. C., & Furman, R. E. (1984) *J. Cell. Biochem.* 26, 135.
- Barhanin, J., Pauron, D., Lombet, A., Norman, R. I., Vijverberg, H. P. M., Giglio, J., & Lazdunski, M. (1983a) *EMBO J.* 2, 915.
- Barhanin, J., Schmid, A., Lombet, A., Wheeler, K. P., Lazdunski, M., & Ellory, J. C. (1983b) *J. Biol. Chem.* 258, 700.
- Barrantes, F. J. (1975) *Biochem. Biophys. Res. Commun.* 62, 407.
- Beneski, D. A., & Catterall, W. A. (1980) *Proc. Natl. Acad. Sci. U.S.A.* 77, 639.
- Catterall, W. A., Morrow, C. S., & Hartshorne, R. P. (1979) *J. Biol. Chem.* 254, 11379.
- Chang, C. T., Wu, C.-S., & Yang, J. T. (1978) *Anal. Biochem.* 91, 13.
- Chen, G. C., & Yang, J. T. (1977) *Anal. Lett.* 10, 1195.
- Clamp, J. R., Bhaffi, T., & Chambers, R. E. (1972) in *The Glycoproteins* (Gottschalk, A., Ed.) pp 300-325, Elsevier, Amsterdam.
- Darbon, H., Jover, E., Couraud, F., & Rochat, H. (1983) *Biochem. Biophys. Res. Commun.* 115, 415.
- Del Valle, U., & Shiveley, J. E. (1979) *Anal. Biochem.* 96, 77.
- Ellisman, M. H., Agnew, W. S., Miller, J. A., & Levinson, S. R. (1982) *Proc. Natl. Acad. Sci. U.S.A.* 79, 4461.
- Ellisman, M. H., Miller, J. A., & Agnew, W. S. (1983) *J. Cell Biol.* 97, 1834.
- Forte, T. M., Nichols, A. V., Gong, E. L., Lux, S., & Levy, R. I. (1971) *Biochim. Biophys. Acta* 248, 381.
- Grishin, E. V., Kovalenko, V. A., Pashikov, V. N., & Shamotienko, G. (1984) *Biol. Membr.* 1, 858.
- Hamilton, R. L., Havel, R. J., Kane, J. P., Blaurock, A. E., & Sata, D. (1971) *Science (Washington, D.C.)* 172, 475.
- Hanke, W., Boheim, G., Barhanin, J., Pauron, D., & Lazdunski, M. (1984) *EMBO J.* 3, 509.
- Hartshorne, R. P., & Catterall, W. A. (1981) *Proc. Natl. Acad. Sci. U.S.A.* 78, 4620.
- Hartshorne, R. P., & Catterall, W. A. (1984) *J. Biol. Chem.* 259, 1667.
- Hartshorne, R. P., Messner, D. J., Coppersmith, J. C., & Catterall, W. A. (1982) *J. Biol. Chem.* 257, 13888.
- Hartshorne, R. P., Keller, B. U., Talvenheim, J. A., Catterall, W. A., & Montal, M. (1985) *Proc. Natl. Acad. Sci. U.S.A.* 82, 240.
- Henderson, R., & Unwin, P. N. T. (1975) *Nature (London)* 257, 28.
- Howell, J. I., Lucy, J. A., Pirola, R. C., & Bouchier, I. A. D. (1970) *Biochim. Biophys. Acta* 210, 1.
- Jover, E. (1984) These d'Etat, Universite d'Aix-Marseille, Faculte de Medecine-Nord.
- Laemmli, U. K. (1970) *Nature (London)* 227, 680.
- Laggner, P., Gotto, A. M., & Morrisett, J. D. (1979) *Biochemistry* 18, 164.
- Levinson, S. R., Curatalo, C. J., Reed, J. K., & Raftery, M. A. (1979) *Anal. Biochem.* 99, 72.

- Mao, D., & Wallace, B. A. (1984) *Biochemistry* 23, 2667.
- Mao, D., Wachter, E., & Wallace, B. A. (1982) *Biochemistry* 21, 4960.
- Massey, J. B., Rhode, M. F., Van Winkle, W. B., Goto, A. M., & Pownall, H. J. (1981) *Biochemistry* 20, 1569.
- Miller, J. A., Agnew, W. S., & Levinson, S. R. (1983) *Biochemistry* 22, 462.
- Moore, W. M., Holladay, L. A., Puett, D., & Brady, R. N. (1974) *FEBS Lett.* 45, 145.
- Morrisett, J. D., Gallagher, J. G., Aune, K. C., & Gotto, A. M. (1974) *Biochemistry* 13, 4765.
- Noda, M., Shimizu, S., Tanabe, T., Takai, T., Kayano, T., Ideda, T., Takahashi, H., Nakayama, H., Kanaoka, Y., Minamino, N., Kangawa, K., Matsuo, H., Raftery, M. A., Hirose, T., Inayama, S., Hayashida, H., Miyata, T., & Numa, S. (1984) *Nature (London)* 312, 121.
- Peterson, G. L. (1977) *Anal. Biochem.* 83, 346.
- Provencher, S. W., & Glockner, J. (1981) *Biochemistry* 20, 33.
- Rosenberg, R. L., Tomiko, S. A., & Agnew, W. S. (1984) *Proc. Natl. Acad. Sci. U.S.A.* 81, 5594.
- Scott, D. A., Smith, K. E., O'Brien, B., & Agelides, K. J. (1985) *J. Biol. Chem.* 259, 10736.
- Tamkun, M. M., & Catterall, W. A. (1981) *J. Biol. Chem.* 256, 11457.
- Waechter, C. J., Schmidt, J. W., & Catterall, W. A. (1983) *J. Biol. Chem.* 258, 5117.
- Wallace, B. A., & Mao, D. (1984) *Anal. Biochem.* 142, 317.
- Weigle, J. B., & Barchi, R. L. (1982) *Proc. Natl. Acad. Sci. U.S.A.* 79, 3651.
- Wray, M., Boulikas, T., Wray, J., & Hancock, R. (1981) *Anal. Biochem.* 118, 187.
- Yager, P., Chang, E. L., Williams, R. W., & Dalziel, A. W. (1984) *Biophys. J.* 45, 26.
- Yuan, P.-M., Pande, H., Clark, B. R., & Shiveley, J. E. (1982) *Anal. Biochem.* 120, 289.
- Zingsheim, H.-P., Neugebauer, D.-C., Frank, J., Hanicke, W., & Barrantes, F. J. (1982) *EMBO J.* 1, 541.

## Methylation of the Active-Site Lysine of Rhodopsin<sup>†</sup>

Colin Longstaff and Robert R. Rando\*

Department of Pharmacology, Harvard Medical School, Boston, Massachusetts 02115

Received June 20, 1985

**ABSTRACT:** Purified bovine rhodopsin was reductively methylated with formaldehyde and pyridine/borane with the incorporation of approximately 20 methyl groups in the protein. Rhodopsin contains 10 non-active-site lysines, which account for the uptake of the 20 methyl groups. The permethylated rhodopsin thus formed is active toward bleaching, regeneration with 11-*cis*-retinal, and the activation of the GTPase (G protein) when photolyzed. The critical active-site lysine of permethylated rhodopsin can be liberated by photolysis. This lysine can be reductively methylated at 4 °C. Methylation under these conditions leads to the incorporation of approximately 1.5 methyl groups per opsin molecule using radioactive formaldehyde, with the ratio of  $\epsilon$ -dimethyllysine: $\epsilon$ -monomethyllysine:lysine being approximately 5:4:1. The modified opsin(s) can regenerate with 11-*cis*-retinal to produce a mixture of active-site methylated and unmethylated rhodopsins having a  $\lambda_{\max}$  = 512 nm. Using [<sup>14</sup>C]formaldehyde and [<sup>3</sup>H]retinal followed by reduction of the Schiff base, digestion, and chromatography showed that the active-site *N*-methyllysine was bound to the retinal. Treatment of the methylated opsin mixture (containing 1.5 active-site methyl groups) with *o*-phthalaldehyde/mercaptoethanol to functionalize the opsin bearing unreacted lysine, followed by regeneration with 11-*cis*-retinal and chromatographic separation, led to the preparation of the pure active-site  $\epsilon$ -lysine monomethylated rhodopsin with a  $\lambda_{\max}$  = 520 nm, significantly shifted bathochromically from rhodopsin or permethylated rhodopsin. Thus, the active site of rhodopsin can accommodate a methyl group attached to the active-site lysine, and the  $\lambda_{\max}$  of this pigment supports the hypothesis that the Schiff base of rhodopsin bears a full formal positive charge. Furthermore, since this new pigment can be bleached, it must mean that deprotonation of the Schiff base must not be obligate for this conversion to proceed. With this methyl reporter group attached to the active-site lysine of rhodopsin, spectroscopic and biochemical experiments on the role of charge and charge movement in the mechanism of action of rhodopsin can be performed.

**R**hodopsin is an integral rod outer segment disk protein containing 11-*cis*-retinal bound to active-site lysine-296 via a protonated, or partially protonated, Schiff base (Hargrave et al., 1983). Photolysis of rhodopsin results in the isomerization of the 11-*cis* chromophore to its all-*trans* congener, with the subsequent hydrolysis of the Schiff base linkage, to form the protein opsin and all-*trans*-retinal (Wald, 1968). One of the spectroscopically identifiable intermediates on the way to

all-*trans*-retinal formation, probably metarhodopsin II, is responsible for initiating the cascade of biochemical events which leads to the hyperpolarization of the rod outer segment, and hence to visual signal transduction (Parkes et al., 1979; Calhoun et al., 1981). It should be noted that metarhodopsin II may be comprised of several distinct conformers. The biochemical events affected by the photochemical activation of rhodopsin are now at least partially understood. Activated rhodopsin (metarhodopsin II) catalyzes the exchange of GTP for GDP in a G protein (GTPase), also called transducin, which can then in turn activate a phosphodiesterase specific for cGMP (Shinozawa et al., 1979; Fung et al., 1981). There

<sup>†</sup> This work was supported by U.S. Public Health Service Research Grant EY 03624 from the National Institutes of Health.

\* Correspondence should be addressed to this author.